Damage diagnosis in circular structures using Cartesian wavelet analysis: A comparison between two structural signals

A. Mahdian Parrany[a], S. Seifoori[a,*], H. Sharifi[a], and M.J. Khoshgoftar[b]

a. *Department of Mechanical Engineering, Vali-e-Asr University of Rafsanjan, Rafsanjan, Iran.*
b. *Department of Mechanical Engineering, Faculty of Engineering, Arak University, Arak, Iran.*

Abstract. Circular structures are used in a wide variety of engineering mechanisms and devices. In this paper, an effective algorithm on the basis of complex mappings is proposed to identify defects in circular structures using Cartesian damage detection techniques. The efficacy of the proposed algorithm is demonstrated through damage identification in circular plates using Cartesian wavelet analysis. The vibration and thermal responses of the structure, as two important structural signals, are imported into the proposed algorithm to evaluate the abilities of the signals to identify the damage location and severity. Finally, two experimental tests are conducted to explore the efficacy of the proposed algorithm in real applications.

1. Introduction

Nowadays, circular structures are widely used in many engineering mechanisms and devices. Circular plates, a type of circular structures, are widespread components in many engineering structures such as diaphragms of steam turbines, nozzle covers, disks of compressors, disks of couplings and clutches, and bulkheads in submarines and airplanes. Hemispherical shells, another type of circular structures, are commonly used as end closures in pressure vessels and storage tanks. These structures are susceptible to defects, like wall-thinning or erosion, because they are usually exposed to severe environmental conditions. Therefore, finding an efficient damage diagnosis algorithm for circular struc-

tures seems essential in order to identify the damages at their early stage of development and prevent sudden failure. In recent years, only a few researchers have studied damage identification in circular structures [1–6].

Frank Pai et al. [1] presented the analytical dynamic characteristics of a circular aluminum plate with a free outer rim and a clamped inner rim using two methods: one used the multiple-shooting method and the other used Bessel functions. The small defects in circular plates could be identified in experimental tests by the boundary effect detection method, which is a non-destructive dynamics-based method. Also, they proposed a new concept using the balance of elastic and kinetic energies within a mode cell for detecting defects in two-dimensional (2D) structures with irregular shapes. Giurgiutiu et al. [2] developed and validated an analytical model for two-dimensional thin-wall structures that predicts the electro-mechanical impedance response at Piezoelectric

---

*. *Corresponding author.*
    E-mail address: sajjad.seifoori@vru.ac.ir (S. Seifoori)

Wafer Active Sensor (PWAS) terminals. The model involves flexural and axial vibrations of the structure and considers both sensor dynamics and structural dynamics. Calibration experiments on circular thin plates with centrally attached PWAS indicated that damage changes the high-frequency electro-mechanical impedance spectrum, resulting in the appearance of new harmonics, peak splitting, and frequency shifts. Trendafoilova et al. [3] investigated the improvement of vibration-based health monitoring methods for thin circular plates. They presented the idea of using the nonlinear time series and large amplitude vibrations analysis for damage detection in circular plates. The proposed damage detection methodology also explored the possibility to use certain distribution characteristics of phase space points on the attractor of the system. Katunin [4] applied the polar wavelet transform to modal shapes to detect and identify external and internal damages to composite structures with circular geometry. The results of comparative study showed that damage detectability were strongly dependent on selecting an appropriate type of wavelet. Praisach et al. [5] investigated changes in natural frequency when damage appears in circular clamped plates. They demonstrated that the curve shape did not change by increasing the damage angle, while the frequency ratio increased. They also showed that the frequency change was insignificant in higher vibration modes, when damage was located at the center of a circular plate. Salmi et al. [6] studied damage identification in the adhesion between a metal hemisphere and a polymer base in case only the rim was accessible. They conducted a series of experiments on a 5 cm diameter metal hemisphere attached to a polymer base and could detect the damage location using a laser Doppler vibrometer and a guided ultrasonic wave (Lamb quasi-modes) generated from the rim of the shell.

The key point is that there are many effective damage detection techniques in the literature, which are suitable for rectangular structures in the Cartesian coordinates [7–12]. Most of these techniques are not directly applicable to circular structures, and it is also very difficult to extend them to the polar coordinates. Ganguli [7] introduced various methods for structural health monitoring and damage detection in aerospace, civil, and mechanical structures in the presence of model uncertainty. Modal curvature-based damage detection, wavelet-based damage detection, fractal dimension-based damage detection, as well as the application of fuzzy logic and probability theory in damage detection were presented. Ghannadi and Kourehli [9] combined modal test analysis model with Artificial Neural Networks (ANN) to propose an effective method for damage assessment based on limited measured locations in skeletal structures. The modal test analysis model was utilized to estimate the unmeasured degrees of freedom and unmeasured mode shapes, while an artificial neural network was trained to estimate the damage characteristics. Numerical simulations indicated high accuracy for structural damage detection. Seifoori et al. [11] studied the behavior of curved composite laminates under low-velocity impact loads. The area of the damaged zone and time history of the mid-point deflection of the laminate due to the impact were considered as two important indices, and the effect of the shape of the impactor nose on the behavior of the curved composite laminate was probed. Gogolewski [13] diagnosed the surface texture of machine parts using fractional spline wavelets. Additive technology and face milling were utilized to prepare the surface profiles of samples. The effects of scaling function order and decomposition level on filtration process were examined, and a comparison between the results of fractional spline wavelet and one-dimensional discrete wavelet transform was conducted. Katunin and Przystałka [14] applied the fractional discrete wavelet transform to the vibration mode shapes of composite plates for damage detection and localization. They used heuristic optimization algorithms to tune the values of wavelets' parameters and improve the sensitivity of the method. Several numerical and experimental tests were conducted to assess the effectiveness of the method. More recently, Shi et al. [15] presented a damage detection strategy based on the two-dimensional directional continuous wavelet transform of mode shapes for identifying line-type damages in plate structures. They evaluated the influence of line-type damages on plate vibration behavior by an analytical long narrow notch-type damage model for simply-supported plates. By employing the excitation-response system of the Scanning laser Doppler Vibrometers and Piezoelectric Leadzirconate-Titanate, an experimental modal test on an artificially induced notched aluminum alloy clamped plate was conducted to assess the practicability and efficiency of the presented algorithm. Hassani et al. [16] developed a novel optimization problem for defect identification of structures with closely spaced eigenvalues. They introduced a mode shape sensitivity-based cost function for defect assessment. Two spatial trusses with multiple damaged elements were considered as case studies, and it was shown that the proposed method had better performance than some previous methods. Zhang et al. [17] introduced an iterative partition method based on waveform centroid in order to locate damage sites in a plate using a few sensors. The performance of the method was assessed by performing several experiments on an aluminum alloy plate using four piezoceramics to act as exciters and receivers and the Lamb waves to scan the plate structure. Song et al. [18] used the fuzzy entropy and singular spectrum analysis to establish an innovative algorithm

for damage detection in thin plates. To generate and detect the Lamb waves, the lead zirconate titanate transducers were employed. The singular spectrum analysis was used to decompose and reconstruct the sensing data and the normalized fuzzy entropy was considered as an index for damage severity. They also designed an experimental setup for an aluminium plate to evaluate the performance of the presented algorithm. Li et al. [19] proposed damage detection algorithm using strain mode differences and the inverse finite element method based on convolutional neural networks. They considered the strain mode differences contaminated by random noises as the input data of the convolutional neural network and demonstrated the acceptable efficiency of the proposed algorithm. Hu et al. [20] presented an innovative algorithm for defect identification based on Lamb waves. The algorithm included two defect measures based on the amplitudes of low-frequency signal direct wave and high-frequency signal maximum component. Numerical simulations and experimental tests on steel plates with various defect depths showed that the algorithm was sensitive to defect depth. Xu et al. [21] used the model updating technique and the estimation of distribution algorithm for defect identification in a single-layer cylindrical latticed shell. Numerical and experimental results demonstrated the effectiveness of the presented defect detection algorithm in the presence of noise interference and multiple damage conditions. It was also shown that the average detection accuracy of the numerical and experimental data was over 90% and 82%, respectively. It is worth mentioning that all of the damage detection algorithms presented in the above cited papers are applicable only for rectangular structures at the Cartesian coordinates.

Meanwhile, it is well known that the input of most of the existing damage detection techniques is a physical signal obtained from the structure. In addition, there is a basic principle expressing that any anomaly alters the physical characteristics of the structure locally. In this regard, it has been proven that the vibration mode shapes and thermal responses of the structure are two efficient signals for damage detection [22–29]. Seifoori et al. [29] presented an experimental study on damage intensity in rectangular composite plates under low-velocity impacts. They used infrared thermography with hot airflow, infrared thermography with a heating element, and ultrasonic vibrothermography for damage detection and evaluation. The wavelet analysis was employed to locate the damage in the thermography images in which the damage was not observable. The experiments demonstrate that the vibrothermography method is the most promising technique for damage evaluation in rectangular composite plates under low-velocity impacts.

The main purpose of this paper is to present an effective algorithm facilitating the application of damage detection techniques, such as the wavelet analysis, at the Cartesian coordinates to circular structures. Another objective of this paper is to compare the damage diagnosis results obtained from vibration mode shapes and thermal responses as two important structural signals in terms of damage detection. The efficacy of the proposed algorithm is evaluated using damage detection in circular plates based on vibrational and thermal responses using the wavelet analysis as a Cartesian damage detection technique. Finally, experimental studies are conducted to verify the effectiveness of the proposed algorithm in real applications. The original contributions and scientific values of this paper are explained as follows:

(i) There is no paper in the literature on damage detection in circular plates using thermal analysis or active thermography;

(ii) This paper establishes a general framework based on the complex mappings for damage detection in circular structures using Cartesian damage detection techniques;

(iii) The damage detection algorithm presented in this paper can be easily extended and applied to other partially regular geometries and shapes.

2. Theoretical background

Since, in this study, the surface temperature distribution and first vibration mode shape of the circular plate are the reference signals for damage diagnosis, the theoretical backgrounds regarding transient thermal analysis and vibration analysis of circular plates are presented in brief. The mathematics of the wavelet analysis is discussed as well.

2.1. Thermal analysis
The theoretical basis of transient thermal analysis for a circular plate using the heat conduction equation can be found in [30,31]. The heat conduction equation must be solved to acquire the temperature distribution of the structure. For a stationary, homogeneous, and isotropic structure, the general form of the heat conduction equation is as the following:

$$\nabla \cdot (k\nabla T) + q = \rho c_p \frac{\partial T}{\partial t}, \tag{1}$$

where k, T, q, ρ, c_p, and t are the thermal conductivity, temperature distribution, rate of internal heat generation, density, specific heat capacity of the structure, and time, respectively. For a circular plate depicted in Figure 1(a) considering no internal heat generation and constant thermal conductivity, the heat conduction
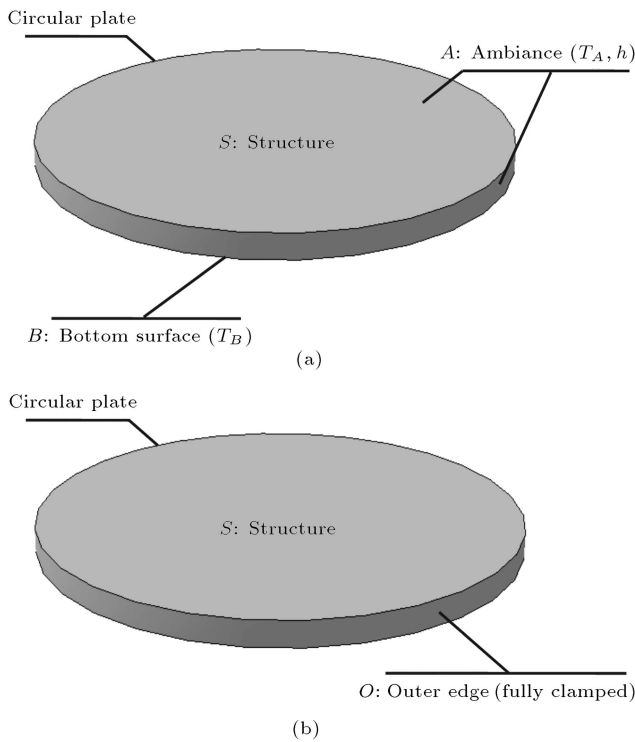
Figure 1. Model of circular plate with (a) Thermal boundary conditions and (b) vibration boundary conditions.

equation governing the temperature distribution of the structure is simplified as follows:

$$k\nabla^2 T = \rho c_p \frac{\partial T}{\partial t} \qquad \text{in} \quad S. \tag{2}$$

The initial and boundary conditions are considered in the following:

$$\begin{cases} k\frac{\partial T}{\partial n} + hT = hT_A & \text{on} \quad A \\ T = T_B & \text{on} \quad B \\ T(t=0) = T_0 & \text{in} \quad S \cup B, \end{cases} \tag{3}$$

where n, h, T_0, T_B, and T_A represent the outward-drawn normal unit vector to the surface, convection heat transfer coefficient, initial temperature, temperature field of the bottom surface, and ambient temperature, respectively. Solving the partial differential equation given in Eq. (2) with the initial and boundary conditions of Eq. (3) yields complete temperature distribution of the circular plate.

2.2. Vibration analysis

The fundamentals of vibration analysis of circular plates can be found in [32]. For the homogeneous and isotropic circular plate shown in Figure 1(b), the governing motion equation for the forced transverse vibration is expressed in the following:

$$D\nabla^4 w + \rho b \frac{\partial^2 w}{\partial t^2} = f \qquad \text{in} \quad S, \tag{4}$$

where D, b, and w denote the flexural rigidity, thickness, and displacement field of the plate, respectively. In addition, f is the distributed transverse load acting on the plate per unit area, which must be replaced by zero in case of the natural mode shapes of the plate. The outer edge of the plate is considered to be fully clamped or fixed as shown in Figure 1(b); thus, the boundary condition can be mathematically represented in the following:

$$w = 0 \qquad \text{on} \quad O. \tag{5}$$

Solving Eq. (4) with the boundary condition presented in Eq. (5) yields the natural vibration mode shapes of the circular plate. In this paper, the surface temperature distribution and first vibration mode shape of circular plate are acquired by employing the ABAQUS software package to develop a three-dimensional finite element model of the structure.

2.3. Wavelet analysis

In this subsection, the mathematical formulation of the wavelet transform is briefly presented. More details can be found in [33–35]. Wavelets are localized waves which have zero mean and drop to zero after a few oscillations. They can be real or complex functions denoted by $\psi(x,y)$. This function is known as the mother wavelet since it is possible to produce a series of wavelet functions $\psi_{s,u,v}(x,y)$ by altering the scale s and the position of the wavelet window in the horizontal and vertical directions (u,v) over the signal in the following:

$$\psi_{s,u,v}(x,y) = \frac{1}{\sqrt{s.s}} \psi\left(\frac{x-u}{s}, \frac{y-v}{s}\right). \tag{6}$$

The 2D Continuous Wavelet Transform (CWT) of the signal $f(x,y)$, which belongs to the Hilbert space of measurable, square-integrable functions, is defined in the following:

$$\begin{aligned} \text{CWT}(s,u,v) &= \langle f, \psi_{s,u,v} \rangle \\ &= \frac{1}{\sqrt{s.s}} \int\limits_{-\infty}^{+\infty}\int\limits_{-\infty}^{+\infty} f(x,y)\psi^*\left(\frac{x-u}{s}, \frac{y-v}{s}\right) dxdy, \end{aligned} \tag{7}$$

where the scale parameter s and the translation parameters u and v are real numbers and $s \neq 0$. Furthermore, $\psi^*(x,y)$ is the complex conjugate of the mother wavelet $\psi(x,y)$, and $CWT(s,u,v)$ is the output of the 2D continuous wavelet transform known as the wavelet detail coefficient. It shows how well a wavelet function correlates with the signal being transformed. Any sudden or sharp discontinuity or irregularity in the signal leads the wavelet detail coefficient to have large magnitudes or local maximums, and it is exactly

the fundamental idea of damage diagnosis using the wavelet analysis. According to the 2D discrete wavelet analysis, the scale and translation parameters are discretized in order to reduce data size and computational time. Although there are several ways of discretization, the most common form of the discrete wavelet analysis, known as the standard Discrete Wavelet Transform (DWT), is formulated as follows:

$$DWT(j,k,m) = \langle f, \psi_{j,k,m} \rangle$$

$$= \frac{1}{2^j} \int\limits_{-\infty}^{+\infty}\int\limits_{-\infty}^{+\infty} f(x,y)\psi^* \left(\frac{x-k2^j}{2^j}, \frac{y-m2^j}{2^j} \right) dxdy, \quad (8)$$

in which j is an integer called the dilation or decomposition level, and k and m are two integers called the translation parameters in the horizontal and vertical directions, respectively. In the literature of the wavelet analysis, there is another important function called the scaling function denoted by $\phi(\circ)$. It is also known as the father wavelet corresponding to the mother wavelet $\psi(\circ)$. In the 2D wavelet transform, based on the separability principle, there are three various wavelet functions as follows:

$$\begin{cases} \psi^V(x,y) = \phi(x)\psi(y) \\ \psi^H(x,y) = \psi(x)\phi(y) \\ \psi^D(x,y) = \psi(x)\psi(y) \end{cases} \quad (9)$$

in which ψ^D, ψ^H, and ψ^V are the diagonal, horizontal, and vertical wavelet functions, respectively. Subsequently, the corresponding wavelet detail coefficients are extracted as follows:

$$\begin{cases} D_j^V(k,m) = \left\langle f, \psi_{j,k,m}^V \right\rangle \\ D_j^H(k,m) = \left\langle f, \psi_{j,k,m}^H \right\rangle \\ D_j^D(k,m) = \left\langle f, \psi_{j,k,m}^D \right\rangle \end{cases} \quad (10)$$

where D_j^D, D_j^H, and D_j^V are known as the diagonal, horizontal, and vertical wavelet detail coefficients at the decomposition level of j, respectively. The wavelet detail coefficients are of great interest and importance since they contain the information necessary to detect irregularities in the signal being transformed.

It is worth mentioning that one of the most crucial shortcomings of signal processing using the wavelet analysis is border and/or boundary distortion. The cause of this issue is that common mechanical systems or civil structures such as beams, plates, and shells have definite boundaries; thus, their corresponding signal begins from a particular point and ends at another particular point. Since the wavelet analysis is the convolution of a wavelet with a signal of finite length, the wavelet detail coefficients will be inevitably distorted by the discontinuity of the input signal at the boundaries. In other words, there is a sudden change at the beginning and end points of the reference signal with a specific length, and the wavelet analysis will identify such variations as an abrupt change. Therefore, the wavelet detail coefficients can reach an extremely high/low value near the boundaries, where proper identification of the damage may be seriously difficult. In recent years, researchers have introduced several techniques to overcome this issue [36–38]. In this study, the reference signal is extended beyond its original boundaries by the cubic spline extrapolation to moderate the undesirable effects of border and/or boundary distortion.

Despite the fact that the selection of an appropriate basis function for the wavelet analysis is still an open problem, there are several well-known mother wavelets that can be effectively used to identify structural anomalies, such as Haar, Daubechies, symlet, and bi-orthogonal wavelets. It is true that all of these wavelets are from orthogonal and bi-orthogonal classes and permit exact reconstruction of the transformed signal, but only Haar and bi-orthogonal wavelets satisfy the symmetry property as a very desirable feature in many applications. Further information about different types of mother wavelets along with their properties, how to select a suitable mother wavelet, and the procedure of structural damage identification by the wavelet analysis was presented in [39]. In this study, the 2D discrete wavelet transform was utilized to identify damage location in circular plates. The first vibration mode shape and surface temperature distribution of the damaged plate are the input signals of the algorithm and decomposed into wavelet detail coefficients using the Haar wavelet at the decomposition level of one. The damage location is shown as a sharp peak in the graphical representation of the wavelet detail coefficients. The magnitude and location of the peak are true measures of the severity and position of the damage, respectively. The wavelet computations are performed in the MATLAB programming environment.

3. Damage diagnosis algorithm

In this section, the algorithm proposed for damage diagnosis in circular structures is described in detail. The main idea is to use the complex mappings. First, the vibrational and thermal signals of the circular structure, which are in the polar coordinates, are transferred into the Cartesian coordinates based on the following complex mapping:

$$x + iy = re^{i\theta}, \quad (11)$$

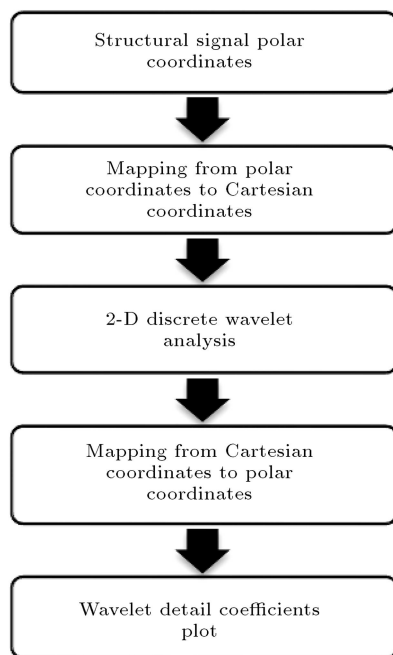where $x-y$ are the Cartesian coordinates, $r-\theta$ are the polar coordinates, and i is the imaginary unit. Now,

Figure 2. Damage diagnosis algorithm for circular structures.

Figure 3. Schematic representation of the damaged circular plate.
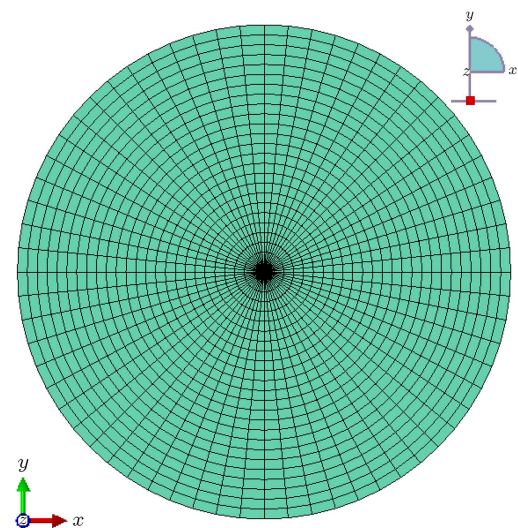
Figure 4. Meshed model of the damaged circular plate in ABAQUS software.

the vibrational or thermal signal of the structure can be processed by the existing mathematical tools at the Cartesian coordinates, such as the 2D discrete wavelet transform. Since then, the results of the analysis, such as 2D wavelet detail coefficients, are turned back into the polar coordinates using the inverse mapping of Eq. (11). The plot of the wavelet detail coefficients in the polar coordinates clearly shows the damage location. Using this algorithm, the horizontal, vertical, and diagonal wavelet detail coefficients at the Cartesian coordinates correspond to the radial, angular, and coupled wavelet detail coefficients in the polar coordinates, respectively. Figure 2 represents the flowchart of the described damage diagnosis algorithm in five steps. The most important advantage of the described damage diagnosis algorithm over the previously used ones is that it can be easily extended and applied to other regular geometries and shapes, such as elliptical structures, by redesigning the complex mapping in Eq. (11). This algorithm enables us to apply all of the existing damage diagnosis techniques at the Cartesian coordinates to circular structures. Moreover, due to the use of the wavelet analysis in the algorithm, no information regarding the intact structure is required. The numerical differentiation of the input signal is not necessary as well.

4. Numerical studies

In this section, two case studies are conducted to evaluate the efficacy of the proposed algorithm for damage diagnosis in circular plates. In the first case
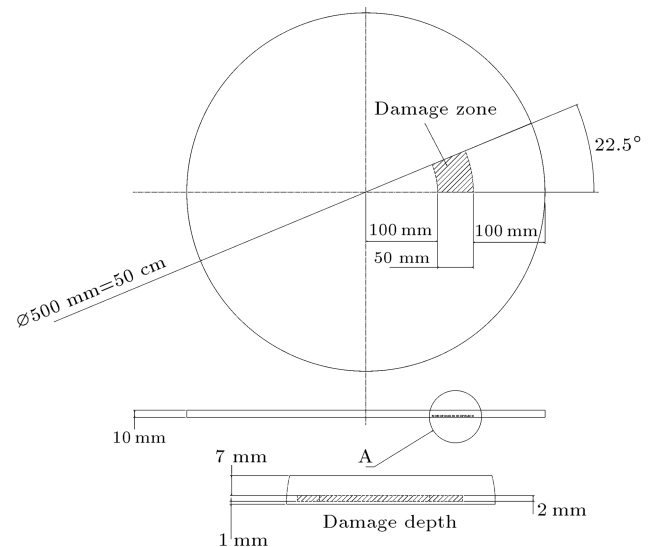
study, the input signal of the algorithm is the steady-state thermal response of a damaged circular plate made of steel. In the second case study, the first vibration mode shape of the plate is the input signal of the algorithm.

A schematic representation of the damaged circular plate under study is shown in Figure 3. The damage is considered as a local reduction in one of the physical parameters of the plate. The circular plate is modeled in the ABAQUS numerical modeling software package and meshed, as shown in Figure 4. In the thermal and vibrational analyses, the DC3D8 and C3D8R solid finite elements with eight nodes and linear shape functions are utilized for the mesh, respectively. Table 1 lists the physical properties of the plate used in numerical simulations.

Table 1. Physical properties.

Parameter	Value	Parameter	Value
Density (kg/m^3)	7800	Young's Modulus (GPa)	200
Poisson's ratio	0.3	Thermal conductivity (W/m.K)	50
Specific heat capacity (J/kg.K)	450	Ambient temperature (K)	293
Convection coefficient (W/m^2.K)	10	Bottom surface temperature (K)	373
Initial temperature (K)	293		

4.1. Case Study 1: Thermal analysis

In this case study, the steady-state thermal response of the damaged circular plate is exported to the proposed algorithm. Capturing the steady-state thermal response of the plate is very convenient using an infrared camera. In the simulation, the initial temperature of the structure is 293K and in order to excite it thermally, the temperature of the bottom surface of the damaged plate suddenly reaches 373 K, as shown in Figure 1(a). The damage is modeled as a 10% reduction in the thermal conductivity of the plate. The steady-state temperature distribution of the upper surface of the damaged circular plate is shown in Figure 5. It should be noted that identification of the damage location from the steady-state temperature distribution of the plate is not possible. The idea is to apply the proposed damage diagnosis algorithm.

Now, the steady-state temperature distribution of the upper surface of the damaged circular plate is exported to the proposed algorithm. The output of the algorithm is presented in Figure 6. It is clear that the damage location is indicated as a sudden and sharp peak in the plot of the wavelet detail coefficients. Moreover, it can be seen that the radial and coupled wavelet detail coefficients reveal the damage location much easier than the angular detail coefficient does.

4.2. Case Study 2: Vibration analysis

In this case study, the first vibration mode shape of the damaged circular plate is considered as the input of the proposed algorithm. The reason behind choosing the first vibration mode shape is that measuring the first vibration mode shape of the plate is much easier than measuring the higher-order vibration mode shapes. In the simulation, the boundary condition of the plate is defined as its outer edge to be fully clamped, as shown in Figure 1(b). The damage is modeled in the form of 10, 20, and 30% reductions in Young's modulus of the plate. The first vibration mode shape of the damaged circular plate with the 10-percent damage is shown in Figure 7. Similarly, identifying the damage-location from the first vibration mode shape of the plate is not possible, as well. The proposed damage diagnosis algorithm is applied.

Now, the first vibration mode shape of the damaged circular plate is exposed to the proposed algorithm. The output of the algorithm for 10, 20, and 30% damages is presented in Figures 8 to 10, respectively. Likewise, the algorithm reveals the location of the damage as a sudden and sharp peak in the plot of the wavelet detail coefficients. It can be seen that the angular wavelet detail coefficient is not able to clarify the damage location.

From Figure 6 and Figures 8–10, the following conclusions can be drawn:

(i) Comparison between Figure 6 and Figure 8 shows that the damage location can be identified from the wavelet detail coefficients of the thermal response of the structure more easily. This implies that under equal circumstances, the thermal response of the structure is more indicative and promising than the vibration response in terms of damage detection;

(ii) It can be seen that the radial wavelet detail coefficient reveals the damage location more accurately than the angular and coupled wavelet detail coefficients;

(iii) While the angular wavelet detail coefficient of the thermal response slightly magnifies the damage location, it is impossible to find the damage location in the angular wavelet detail coefficients of the vibration response. Therefore, it can be
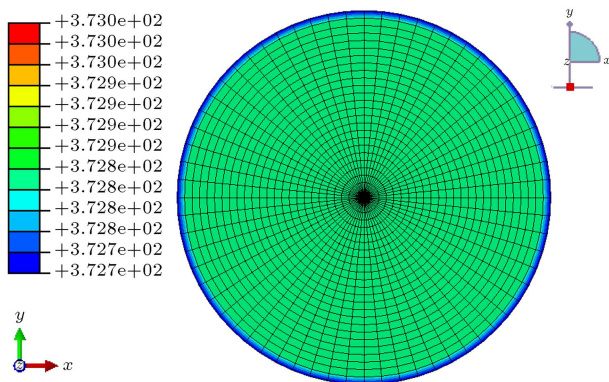

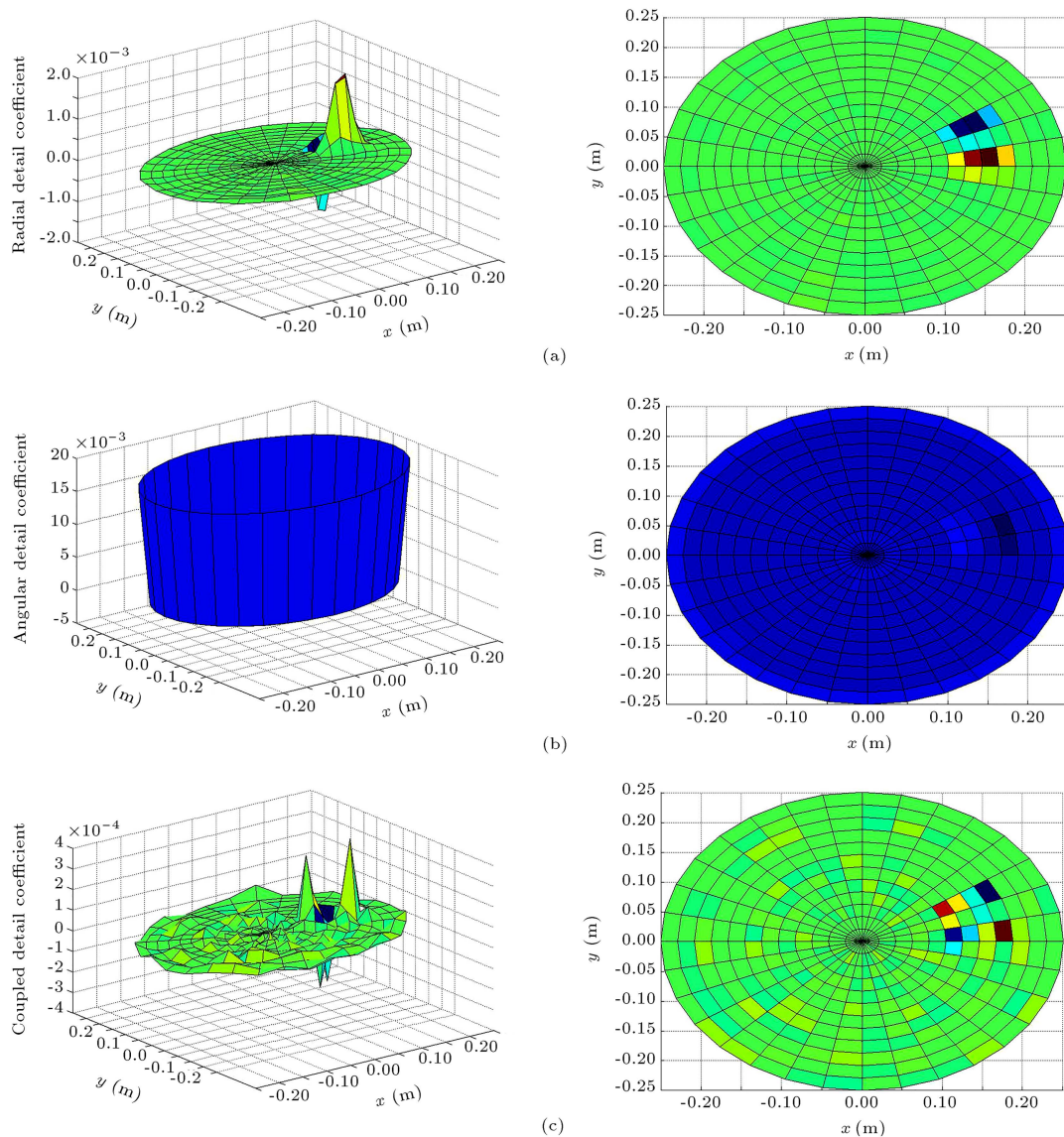**Figure 5.** Steady-state temperature distribution of the damaged circular plate.

Figure 6. Output of the proposed algorithm for case study 1 with 10 percent damage: (a) Radial, (b) angular, and (c) coupled wavelet detail coefficients.
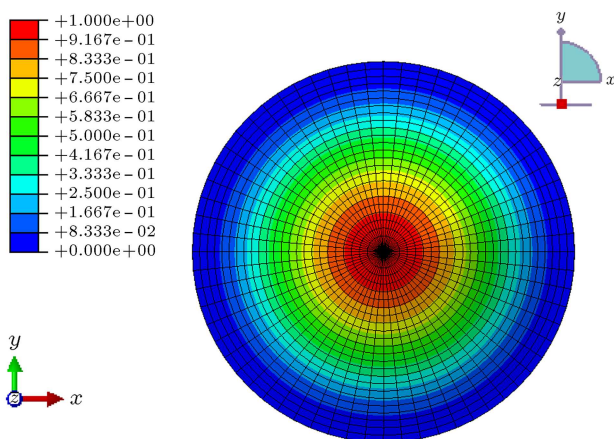

Figure 7. First vibration mode shape of the damaged circular plate.

expressed that the angular wavelet detail coefficient is not entirely useful for damage detection in circular plates;

(iv) In Case Study 2 and Figures 8–10, the maximum values of the radial wavelet detail coefficient for 10, 20, and 30% damages are 1.07e-4, 2.19e-4, and 3.38e-4, respectively. The trend demonstrates that the higher the intensity of the damage, the greater the maximum value of the radial wavelet detail coefficient. In fact, it can be concluded that the maximum value of the radial wavelet detail coefficient can be known as a promising index for evaluating the damage intensity;

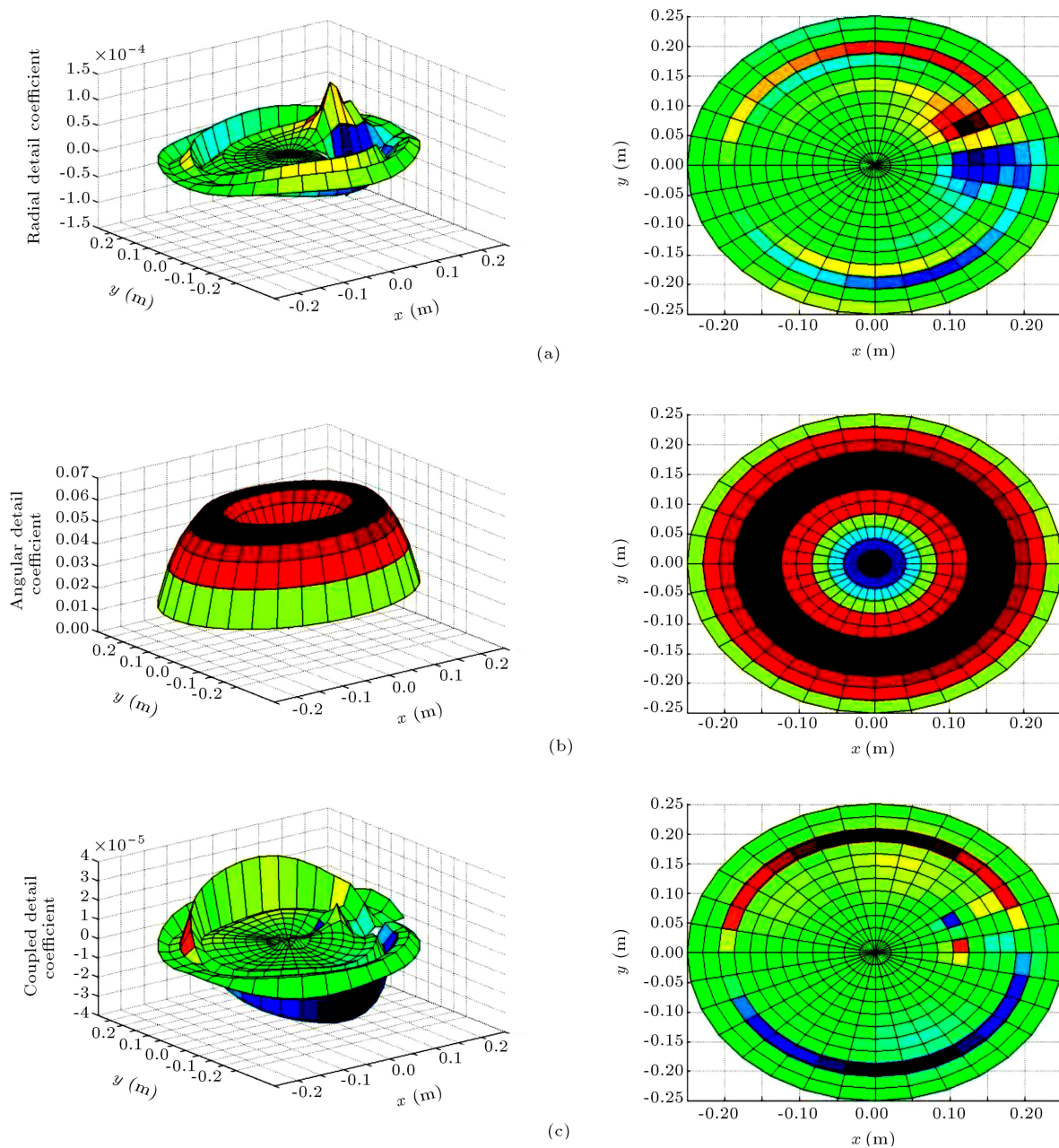(v) Overall, the wavelet detail coefficients, specifically the radial and coupled ones, reveal the damage

Figure 8. Output of the proposed algorithm for Case Study 2 with 10 percent damage: (a) Radial, (b) angular, and (c) coupled wavelet detail coefficients.

location with high accuracy. However, they are not able to estimate the damage size, e.g., depth, width, area, etc. The only decisive fact is that the maximum value of the radial wavelet detail coefficient is an acceptable relative index for evaluating the damage intensity.

5. Experimental studies

In this section, two experimental tests are conducted to investigate the efficacy of the proposed damage detection algorithm in real applications. In the first experiment, the specimen is a circular plate made of

steel, while in the second experiment, the specimen is a circular plate made of Glass Fiber Reinforced Polymer (GFRP) composites.

5.1. Experiment 1: Steel circular plate

In this experimental test, the specimen is a circular plate made of steel with a diameter of 300 mm and a thickness of 10 mm. One side of the plate is intact, while there is square damage as wall-thinning with a depth of 2 mm, as shown in Figure 11. In order to thermally excite the specimen, the damaged side of the plate is exposed to a homogeneous source of energy, i.e., boiling water, while the temperature distribution
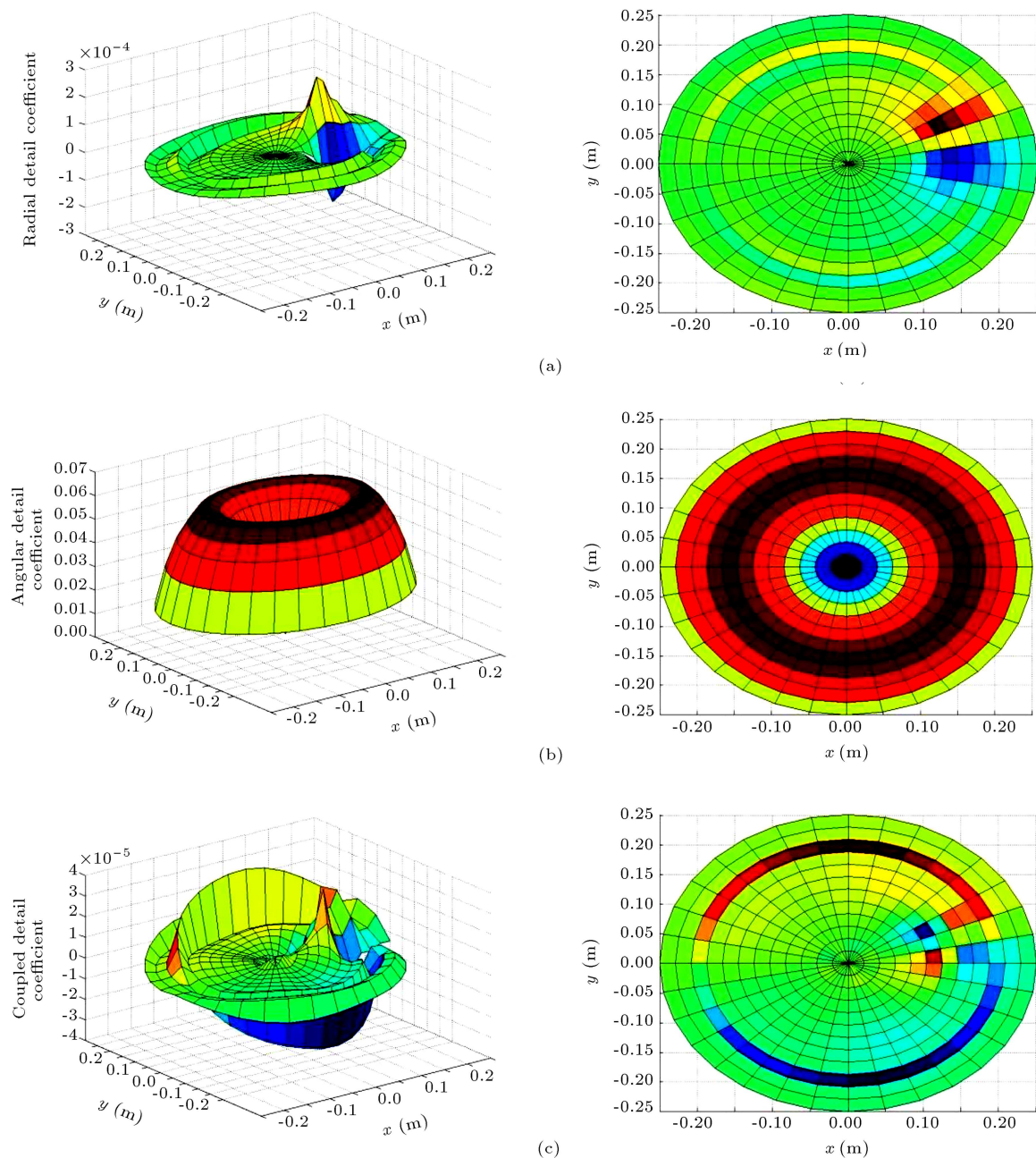
Figure 9. Output of the proposed algorithm for Case Study 2 with 20 percent damage: (a) Radial, (b) angular, and (c) coupled wavelet detail coefficients.

of the intact side of the plate is captured by the infrared (IR) camera FLIR E60.

After 20 minutes of heating the specimen, the thermography image shown in Figure 12 is recorded from the intact surface of the specimen by the infrared camera. It seems natural that it is not possible to find the damage location from the raw thermography image. Since there is no sign of the damage, the idea is to export the temperature distribution of the intact side of the specimen into the proposed damage diagnosis algorithm to magnify the damage location.

In order to extract the temperature distribution

of the intact surface of the specimen from the captured thermography image, the circular shape in Figure 12 manually meshes into a grid of $20 * 32$ elements along the radial and circumferential directions, as shown in Figure 13.

Now, the temperature of the nodes generated by the meshing is manually extracted and imported into the proposed damage diagnosis algorithm. The output of the algorithm is reported in Figure 14.

It is obvious that the plots of the radial and coupled wavelet detail coefficients reveal the damage location, but there is no clear sign of the damage
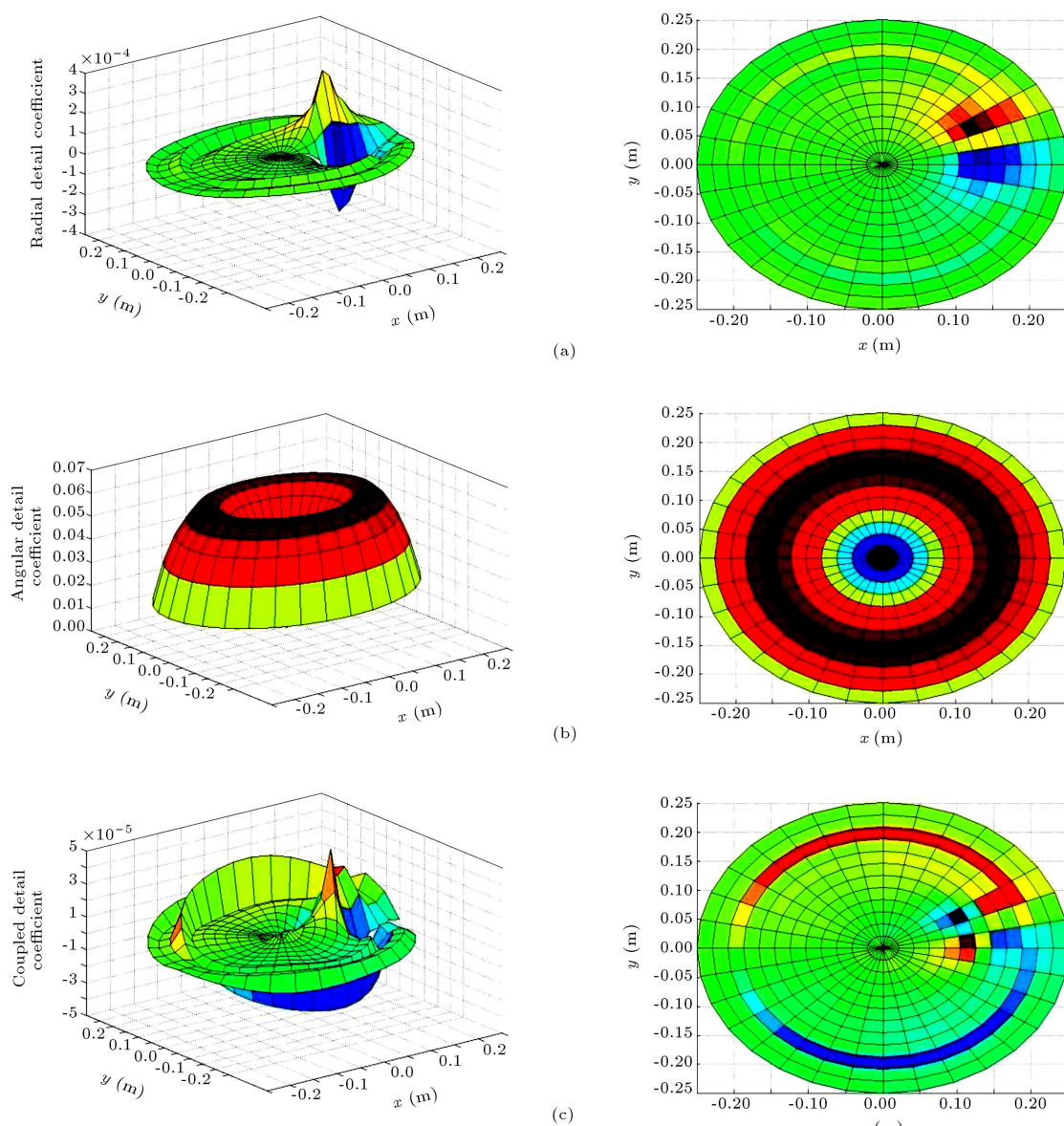
Figure 10. Output of the proposed algorithm for Case Study 2 with 30 percent damage: (a) Radial, (b) angular, and (c) coupled wavelet detail coefficients.
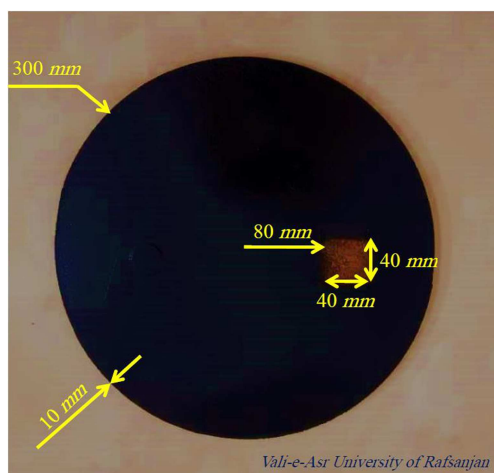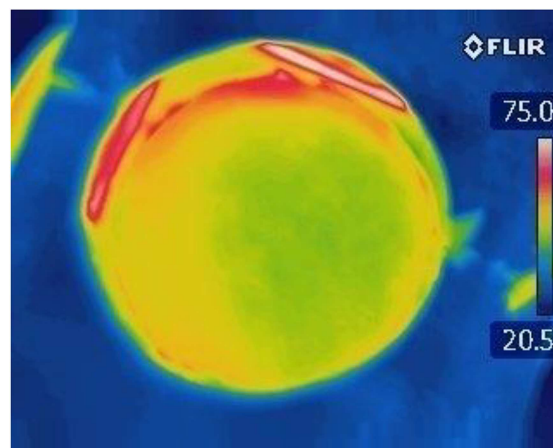

Figure 11. Experimental specimen made of steel.

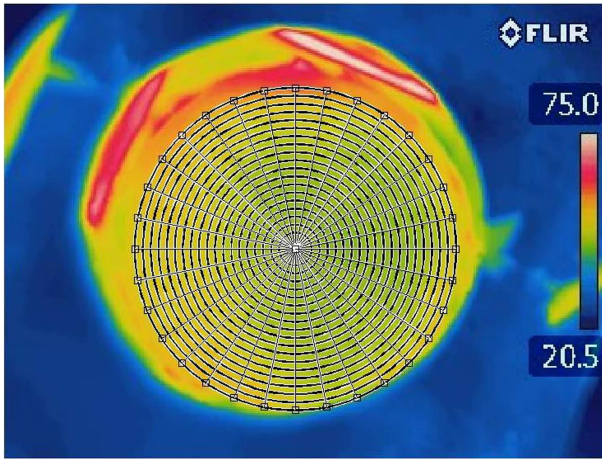**Figure 12.** Thermography image of the specimen made of steel.

**Figure 13.** Meshed diagram of circular shape in the thermography image of the specimen made of steel.

location in the plot of the angular wavelet detail coefficient. This is consistent with the theoretical findings presented in the previous section. It is worth mentioning that while the damage location is shown as a summit in the plot of the radial wavelet detail coefficient, it is depicted as a valley in the plot of the coupled wavelet detail coefficient.

### 5.2. Experiment 2: Composite circular plate

In this experimental test, the specimen is a circular plate made of glass fiber reinforced polymer composites with a diameter of 300 mm and a thickness of 3 mm. The composite laminate is manufactured by the hand lay-up method [40] with the configuration of $[0/90]_{15}$. The top and bottom $[0/90]_5$ laminates of the specimen are intact, while there is a circular hole with a diameter
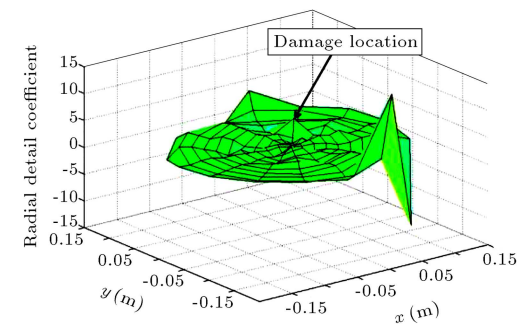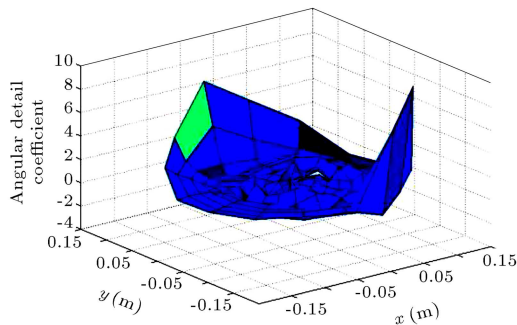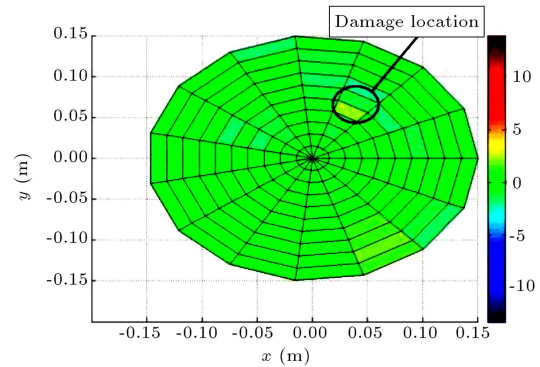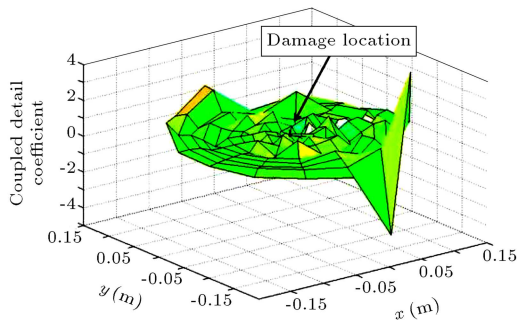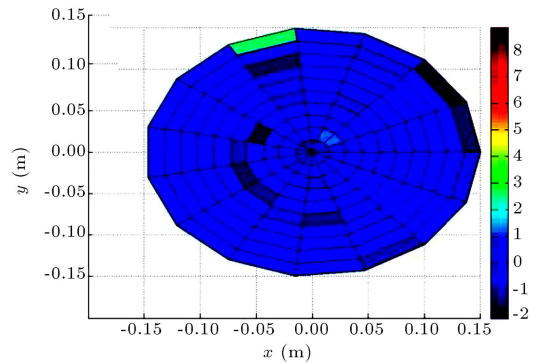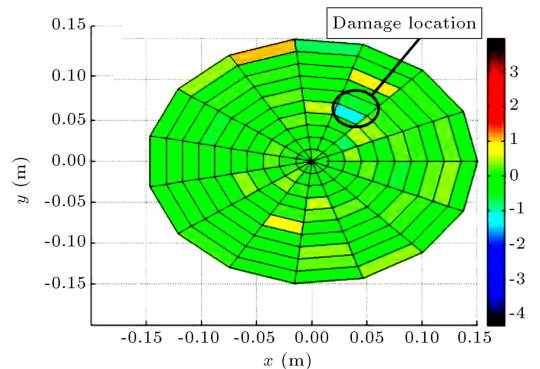

Figure 14. Output of the proposed algorithm for experimental specimen made of steel: (a) Radial, (b) angular, and (c) coupled wavelet detail coefficients.
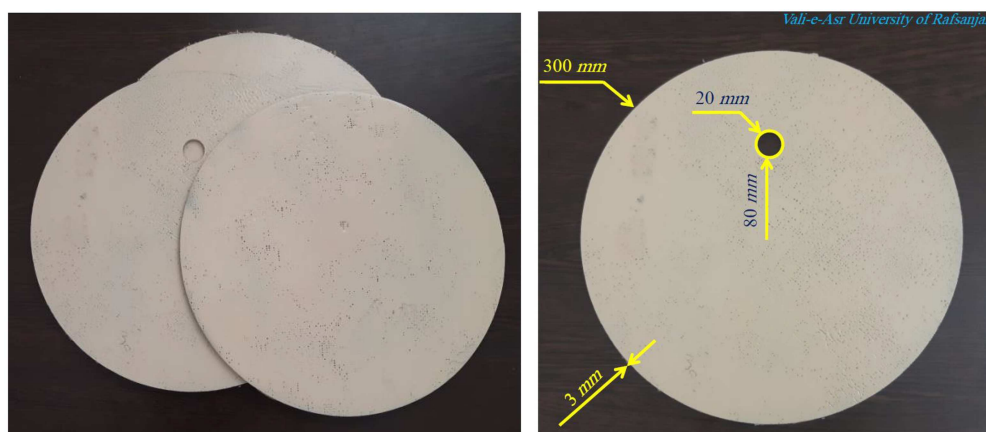
Figure 15. Experimental specimen made of GFRP composites.

Figure 16. Experimental setup for specimen made of GFRP composites.
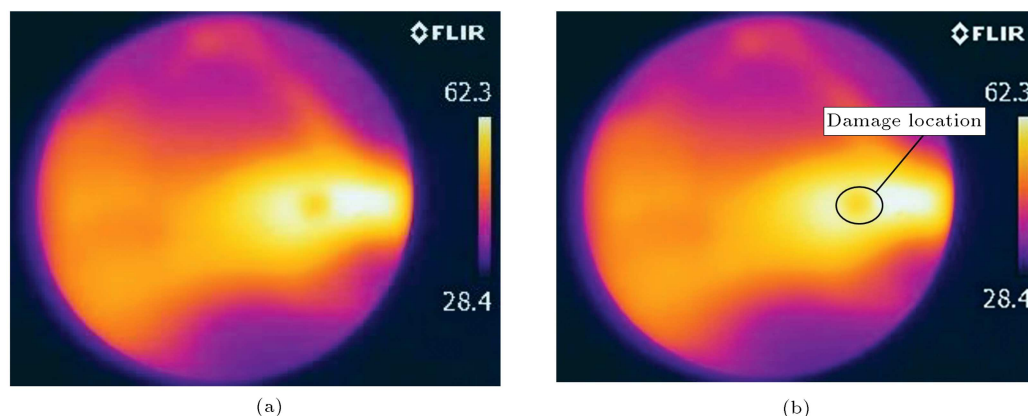

Figure 17. Thermography image of the specimen made of GFRP composites: (a) Raw thermography image and (b) thermography image with damage location.

of 20 mm in the mid $[0/90]_5$ laminate of the specimen, as shown in Figure 15. In order to stimulate the specimen thermally, one side of the specimen is exposed to a homogeneous source of energy, i.e., hot airflow, while the temperature distribution of the other side of the specimen is measured by the infrared (IR) camera FLIR E60. Figure 16 describes the designed experimental setup.

After 10 minutes of heating the specimen, the IR camera captures the thermography image shown in Figure 17(a). Although, in this experiment, it is possible to guess the damage location from the raw thermography image as shown in Figure 17(b), there might exist some sort of uncertainty in the location of the damage, especially for damages with lower intensity. The proposed damage diagnosis algorithm helps
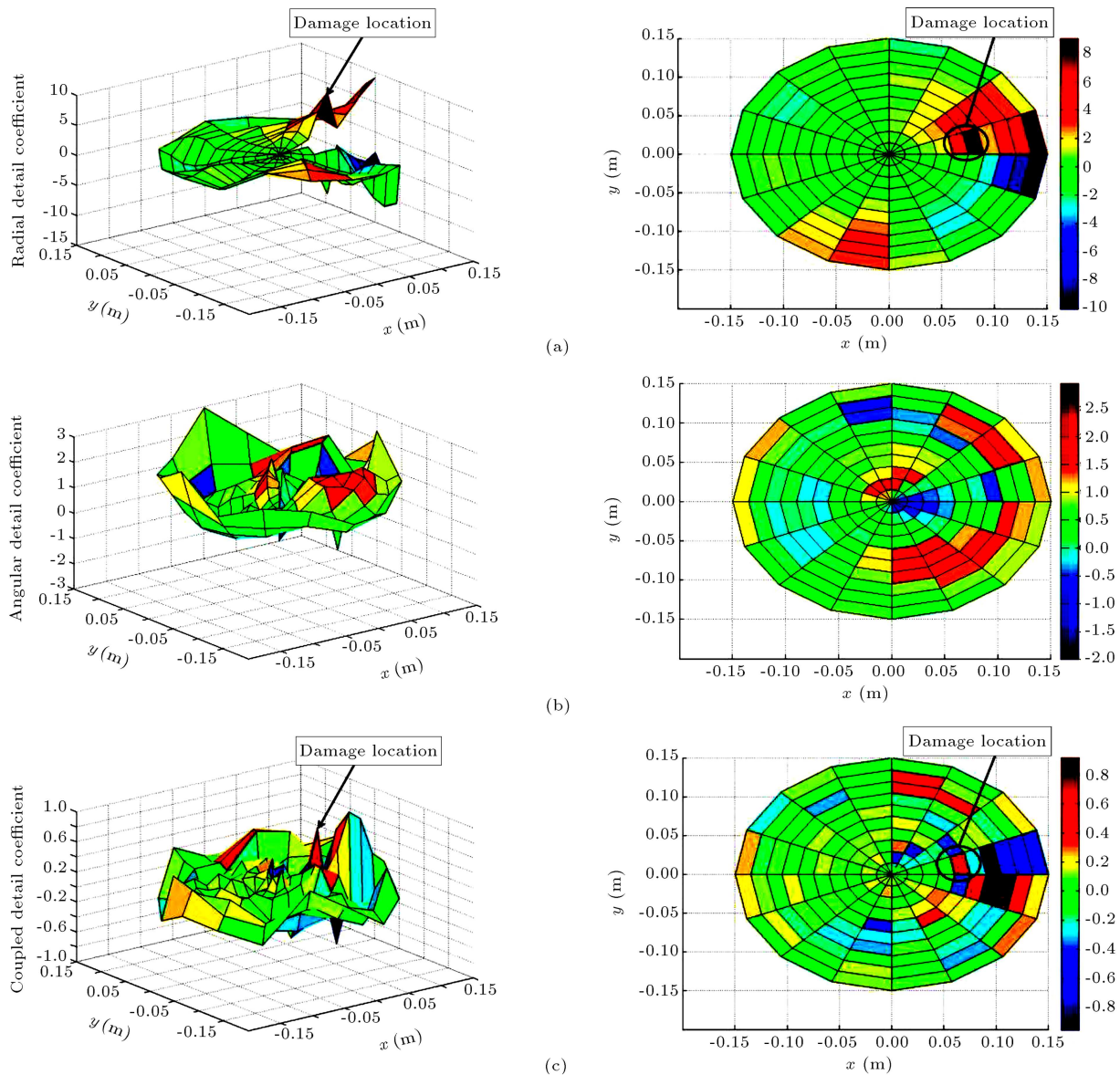
Figure 18. Output of the proposed algorithm for the experimental specimen made of GFRP composites: (a) Radial, (b) angular, and (c) coupled wavelet detail coefficients.

determine the damage location with higher accuracy and certainty.

The temperature distribution of the specimen is extracted by the method described in the previous subsection and then, imported into the proposed damage diagnosis algorithm. The output of the algorithm is shown in Figure 18.

It is evident that the plots of the wavelet detail coefficients magnify the damage location and ensure the inspector about the location of the damage with higher certainty and accuracy. As can be seen, there are a lot of fluctuations in the plot of the wavelet detail coefficients, mainly due to the noise. The noise level in the thermography image depends on the precision and calibration of the IR camera. It is well known

that using a high-precision camera helps process and analyze the images with more reliability.

5.3. Error analysis

In this subsection, an error analysis is conducted to examine the precision of the employed IR camera by making a comparison between the numerical and experimental results. The specimen made of steel and shown in Figure 11 is considered again. Figure 19(a) reports the plot of the temperature distribution along the reference axis $O-r$ drawn in Figure 19(b). It is obvious that there is good and acceptable agreement between the numerical and experimental results. It is true that there is a noticeable difference between the numerical and experimental results; nevertheless, the pattern of
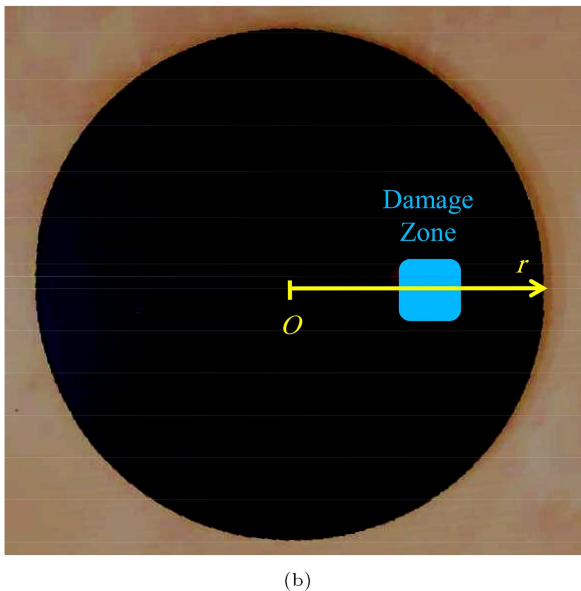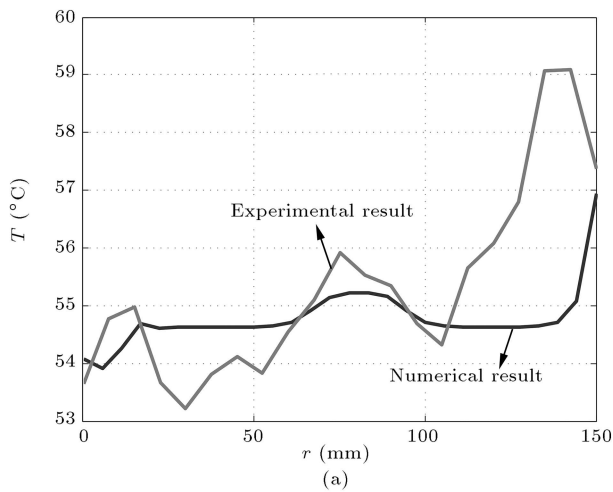
Figure 19. Error analysis of the specimen made of steel: (a) Temperature distribution and (b) reference axis.

temperature variation along the reference axis is quite similar and consistent based on the damage location. The reason behind the mentioned noticeable difference and fluctuations in the experimental plot is the noise in the thermography image. In damage diagnosis applications, it is recommended that a high-precision and carefully calibrated infrared (IR) camera be used.

6. Conclusion and future work

The current paper proposed a simple and efficient algorithm on the basis of the complex mappings for damage diagnosis in circular structures using Cartesian damage detection techniques. In order to demonstrate the efficacy of the proposed damage diagnosis algorithm, a damaged circular plate, as a popular type of circular structures, and the Cartesian wavelet analysis, as a powerful Cartesian damage detection technique, were utilized with the purpose of identifying the damage location in the structure. The thermal and vibrational responses of the structure were used as the inputs of the algorithm, and their abilities were compared from the damage detection point of view. It was found that under equal circumstances, if the thermal response of the structure was imported into the algorithm, the damage location was detected with more accuracy and clarity. It was also concluded that the radial wavelet detail coefficient reveals the damage location more clearly than the angular and coupled wavelet detail coefficients. Additionally, it was shown that the maximum value of the radial wavelet detail coefficient was a promising index of the damage intensity due to the fact that more damage intensity would result in more maximum value for the radial wavelet detail coefficient. Generally, the wavelet detail coefficients, especially the radial and coupled ones, reveal the damage location with high accuracy, but they are not able to estimate the damage size. Finally, some experimental tests based on the active thermography were carried out to validate the efficacy of the algorithm in real applications. The proposed algorithm can be used for damage diagnosis in hemispherical shells as another type of circular structures. Furthermore, the algorithm is so flexible that it can be easily extended and applied to other geometries and shapes, such as elliptical structures, by only redesigning the complex mapping of the algorithm.

Nomenclature

k	Thermal conductivity
T	Temperature distribution
q	Rate of internal heat generation
ρ	Density
c_p	Specific heat capacity
t	Time
n	Outward drawn normal unit vector to surface
T_0	Initial temperature
T_B	Temperature field of bottom surface
T_A	Ambient temperature
h	Convection heat transfer coefficient
D	Flexural rigidity
b	Thickness
w	Plate displacement field
f	Distributed transverse load per unit area
$\psi(x, y)$	Mother wavelet
u	Position of wavelet window in horizontal direction
v	Position of wavelet window in vertical directions

s	Scale of wavelet window
$\psi^*(\circ,\circ)$	Complex conjugate of mother wavelet
$CWT(s,u,v)$	Wavelet detail coefficients
j	Dilation or decomposition level
k	Translation parameter in horizontal directions
m	Translation parameter in vertical directions
$\phi(\circ)$	Scaling function or father wavelet
ψ^V	Vertical wavelet function
ψ^H	Horizontal wavelet function
ψ^D	Diagonal wavelet function
D_j^V	Vertical wavelet detail coefficient at the decomposition level of j
D_j^H	Horizontal wavelet detail coefficient at the decomposition level of j
D_j^D	Diagonal wavelet detail coefficient at the decomposition level of j
$x-y$	Cartesian coordinates
$r-\theta$	Polar coordinates
i	Imaginary unit

References

1. Frank Pai, P., Oh, Y., and Lee, S.-Y. "Detection of defects in circular plates using a scanning laser vibrometer", *Structural Health Monitoring*, **1**(1), pp. 63–88 (2002).

2. Giurgiutiu, V. and Zagrai, A. "Damage detection in thin plates and aerospace structures with the electro–mechanical impedance method", *Structural Health Monitoring*, **4**(2), pp. 99–118 (2005).

3. Trendafoilova, I., Gorman, D.G., and Manoach, E. "An investigation on vibration–based damage detection in circular plates", *Structural Health Monitoring*, **8**(4), pp. 291–302 (2009).

4. Katunin, A. "Vibration–based damage identification in composite circular plates using polar discrete wavelet transform", *Journal of Vibroengineering*, **15**, pp. 355–363 (2013).

5. Praisach, Z.I., Micliuc, D.M., Gillich, G.R., et al. "Natural frequency shift of damaged circular plate clamped all around", *ANNALS of Faculty Engineering Hunedoara – International Journal of Engineering*, Tome XIV – Fascicule, **4**(November), pp. 57–62 (2016).

6. Salmi, A., Heino, O., Nieminen, H.J., et al. "Detecting defects in adhesion between a metal hemisphere and a polymer base", *IEEE International Ultrasonics Symposium (IUS)*, Prague, Czech Republic, pp. 695–698 (2013).

7. Ganguli, R., *Structural Health Monitoring: A Non–Deterministic Framework*, Springer, Singapore (2020).

8. Ostachowicz, W. and Güemes, A., *New Trends in Structural Health Monitoring*, Springer–Verlag Wien, New York (2013).

9. Ghannadi, P. and Kourehli, S.S. "An effective method for damage assessment based on limited measured locations in skeletal structures", *Advances in Structural Engineering*, **24**(1), pp. 1–9 (2021).

10. Tehrani, H.A., Bakhshi, A., and Akhavat, M. "An effective approach to structural damage localization in flexural members based on generalized S–transform", *Scientia Iranica*, **26**(6), pp. 3125–3139 (2019).

11. Seifoori, S., Parrany, A.M., and Mirzarahmani, S. "Impact damage detection in CFRP and GFRP curved composite laminates subjected to low–velocity impacts", *Composite Structures*, **0**, pp. 1–15 (2021).

12. Parrany, A.M. and Mirzaei, M. "A new image processing strategy for surface crack identification in building structures under non–uniform illumination", *IET Image Processing*, **16**(2), pp. 407–415 (2022).

13. Gogolewski, D. "Fractional spline wavelets within the surface texture analysis", *Measurement*, **179**, p. 109435 (2021).

14. Katunin, A. and Przystałka, P. "Damage assessment in composite plates using fractional wavelet transform of modal shapes with optimized selection of spatial wavelets", *Engineering Applications of Artificial Intelligence*, **30**, pp. 73–85 (2014).

15. Shi, B., Cao, M., Wang, Z., et al. "A directional continuous wavelet transform of mode shape for line–type damage detection in plate–type structures", *Mechanical Systems and Signal Processing*, **167**, p. 108510 (2022).

16. Hassani, S., Mousavi, M., and Gandomi, A.H. "A mode shape sensitivity–based method for damage detection of structures with closely–spaced eigenvalues", *Measurement*, **190**, p. 110644 (2022).

17. Zhang, B., Liu, H., Wang, X., et al. "Damage identification in aluminum plates based on iterative partition algorithm using waveform centroid", *Wave Motion*, **108**, p. 102842 (2022).

18. Song, H., Xiang, M., Lu, G., et al. "Singular spectrum analysis and fuzzy entropy–based damage detection on a thin aluminium plate by using PZTs", *Smart Materials and Structures*, **31**(3), pp. 1–8 (2022).

19. Li, M., Jia, D., Wu, Z., et al. "Structural damage identification using strain mode differences by the iFEM based on the convolutional neural network (CNN)", *Mechanical Systems and Signal Processing*, **165**, p. 108289 (2022).

20. Hu, M., He, J., Zhou, C., et al. "Surface damage detection of steel plate with different depths based on Lamb wave", *Measurement*, **187**, p. 110364 (2022).

21. Xu, Y., Pan, Y., Wang, Y., et al. "Damage identification of single–layer cylindrical latticed shells based on the model updating technique", *Journal of Civil Structural Health Monitoring*, pp. 1–15 (2022).

22. Avci, O., Abdeljaber, O., Kiranyaz, S., et al. "A review of vibration–based damage detection in civil structures: From traditional methods to machine learning and deep learning applications", *Mechanical Systems and Signal Processing*, **147**, p. 107077 (2021).

23. Gomes, G.F., Mendez, Y.A.D., Alexandrino, P.D.S.L., et al. "A review of vibration based inverse methods for damage detection and identification in mechanical structures using optimization algorithms and ANN", *Archives of Computational Methods in Engineering*, **26**(4), pp. 883–897 (2019).

24. He, Y., Deng, B., Wang, H., et al. "Infrared machine vision and infrared thermography with deep learning: a review", *Infrared Physics & Technology*, **116**, p. 103754 (2021).

25. Parrany, A.M. "Damage detection in circular cylindrical shells using active thermography and 2–D discrete wavelet analysis", *Thin–Walled Structures*, **136**, pp. 34–49 (2019).

26. Seifoori, S., Izadi, R., and Yazdinezhad, A.R. "Impact damage detection for small– and large–mass impact on CFRP and GFRP composite laminate with different striker geometry using experimental, analytical and FE methods", *Acta Mechanica*, **230**, pp. 4417–4433 (2019).

27. Ghannadi, P. and Kourehli, S.S. "Structural damage detection based on MAC flexibility and frequency using moth–flame algorithm", *Structural Engineering and Mechanics*, **70**(6), pp. 649–659 (2019).

28. Lashkari, A.E. and Firouzmand, M. "Developing a toolbox for clinical preliminary breast cancer detection in different views of thermogram images using a set of optimal supervised classifiers", *Scientia Iranica*, **25**(3), pp. 1545–1560 (2018).

29. Seifoori, S., Izadi, R., Liaghat, G.H., et al. "An experimental study on damage intensity in composite plates subjected to low–velocity impacts", *Polymer Testing*, **93**(106887), pp. 1–14 (2021).

30. Oosthuizen, P.H. and Naylor, D., *Introduction to Convective Heat Transfer Analysis*, WCB/McGraw Hill, New York (1999).

31. Incropera, F.P. and DeWitt, D.P., *Fundamentals of Heat and Mass Transfer*, Wiley, New York (2002).

32. Rao, S.S., *Vibration of Continuous Systems*, John Wiley & Sons, New Jersey (2007).

33. Gao, R.X. and Yan, R., *Wavelets: Theory and Applications for Manufacturing*, Springer, New York (2011).

34. Chui, C.K., *An Introduction to Wavelets*, Academic Press, San Diego (1992).

35. Newland, D.E., *An Introduction to Random Vibrations: Spectral and Wavelet Analysis*, Longman, Harlow and John Wiley, New York (1993).

36. Messina, A. "Refinements of damage detection methods based on wavelet analysis of dynamical shapes", *International Journal of Solids and Structures*, **45**(14–15), pp. 4068–4097 (2008).

37. Fan, W. and Qiao, P. "A 2–D continuous wavelet transform of mode shape data for damage detection of plate structures", *International Journal of Solids and Structures*, **46**(25–26), pp. 4379–4395 (2009).

38. Alamdari, M.M., Li, J., and Samali, B. "Damage identification using 2–D discrete wavelet transform on extended operational mode shapes", *Archives of Civil and Mechanical Engineering*, **15**(3), pp. 698–710 (2015).

39. Ovanesova, A.V. and Suarez, L.E. "Applications of wavelet transforms to damage detection in frame structures", *Engineering Structures*, **26**(1), pp. 39–49 (2004).

40. Seifoori, S., Mirzaei, M., and Afjoland, H. "Experimental and FE analysis for accurate measurement of deflection in CFRP and GFRP laminates under bending", *Measurement*, **153**(107445), pp. 1–8 (2020).

Biographies

Ahmad Mahdian Parrany received his BSc degree in Mechanical Engineering from University of Sistan and Baluchestan, Zahedan, Iran in 2010. He also received his MSc degree in Mechanical Engineering from Amirkabir University of Technology, Tehran, Iran in 2012. He is currently a PhD Candidate of Mechanical Engineering at Sharif University of Technology, Tehran, Iran. His fields of research are structural health monitoring, damage detection, wavelet analysis, dynamic systems, and control.

Sajjad Seifoori received his MSc and PhD degrees from Tarbiat Modares University, Iran in 2014 and BSc from Shahid Bahonar University in Mechanical Engineering. His experience includes an associate professorship at VRU University (academic staff). His fields of research are structural health monitoring, damage detection, wavelet analysis, impact mechanics, and high-speed metal forming. He has contributed about 30 papers and 1 book to the open press.

Hamid Sharifi received his BSc and MSc degrees in Mechanical Engineering from VRU University, Iran in 2020. His fields of research are structural health monitoring, damage detection, and wavelet analysis.

Mohammad Javad Khoshgoftar received his BSc degree in Mechanical Engineering from University of Kashan, Iran. He also received his MSc and PhD degree from Tarbiat Modares University, Iran in 2016 in Mechanical Engineering. He is currently an academic staff member at Arak University. His fields of research are structural health monitoring, damage detection and stress analysis.